

The structure, slip systems, and microhardness of C₆₀ crystals

S. V. Lubenets, V. D. Natsik, L. S. Fomenko, A. P. Isakina, A. I. Prokhvatilov, M. A. Strzhemechny, and N. A. Aksenova

*B. I. Verkin Institute for Low Temperature Physics and Engineering, National Academy of Sciences of the Ukraine, 310164 Kharkov, Ukraine**

R. S. Ruoff

Dept. of Physics, CB 1105, One Brookings Drive, Washington University, St. Louis, MO 63130-4899, USA
(Submitted July 1, 1996; revised September 9, 1996)

Fiz. Nizk. Temp. **23**, 338–351 (March 1997)

The structure and microplasticity of high-purity fullerite C₆₀ have been investigated comprehensively. The crystalline structure, lattice parameters, and phase transitions have been studied by x-ray diffractometry in the temperature range 30–293 K. It is found that the temperature corresponding to the orientational order–disorder phase transition is $T_c = 260$ K. A considerable number of regions with stacking faults discovered in the samples leads to blurring of the fcc→sc phase transition in the temperature interval $T_c \pm 3$ K. The $a(T)$ dependences of the lattice parameter display peculiarities at the following characteristic temperatures: T_c at which the lattice parameter jump $\Delta a/a = 3.3 \times 10^{-3}$ is observed, and the temperatures $T_0 \approx 155$ K, and $T_g \approx 95$ K which are associated with the beginning and end of molecular orientation freezing. It is shown that the formation of orientational glass is accompanied by a considerable increase in the width of x-ray reflections. The slip geometry and the temperature dependence of microhardness H_V are studied in the temperature interval 81–293 K. It is shown that a system of the {111}<110> type is the only slip system in the fcc and sc phases. The value of H_V depends on the indentation plane: $H_V^{111} > H_V^{100}$. Below T_c , the microhardness increases abruptly (by approximately 30%). The temperature interval of this anomaly decreases after annealing of the crystal in vacuum. At $T < T_0$, the $H_V(T)$ dependence becomes much stronger. It is shown that the hardness of C₆₀ normalized to the elastic shear modulus is higher than the hardness of typical molecular crystals at comparable homologous temperatures. © 1997 American Institute of Physics. [S1063-777X(97)01303-0]

1. INTRODUCTION

Fullerite C₆₀ is a typical simple molecular crystal in which peculiarities of lattice properties such as polymorphism are associated with the thermal activity of rotational degrees of freedom of their molecules. The phase transition observed at $T_c = 260$ K (which is a first-order phase transition according to some indications) does not change the symmetry of spatial arrangement of the centers of gravity of molecules that form the fcc lattice. A decrease in lattice symmetry from $Fm\bar{3}m$ (fcc) to $Pa\bar{3}$ (sc) upon cooling is due to partial orientational ordering of molecules.^{1–3} Neutron diffraction studies^{2,4} have revealed that the molecules in the low-temperature phase are in two orientational states that are nonequivalent from the symmetry point of view, but have close energy values. These states are called pentagonal and hexagonal configurations and correspond to global and local energy minima of the noncentral part of molecular interaction. They are separated by the energy gap of ~ 0.25 eV. The number of less advantageous hexagonal configurations decreases upon cooling, but so does the rotational frequency of molecules. Hence the orientational glass phase is formed even at a fairly high temperature ~ 90 K.^{2,4–6} Variations in

the orientational subsystem must influence the temperature dependence of the structural and other physical characteristics of fullerite crystals.

The high-temperature fcc phase of fullerite, which is dominated by central van der Waals molecular interaction, can be formally treated as a “plastic crystal” according to the classification and criteria proposed by Timmermans.⁷ A transition to the orientationally ordered SC phase is accompanied by an enhancement of the role of the off-central component in molecular interaction, and must increase the lattice rigidity. Moreover, a change in the lattice symmetry due to such a transition can lead to a change in the crystallography of plastic slip.⁸ Hence, in addition to structural studies, investigations of the parameters of plastic deformation and slip systems of C₆₀ crystals as well as their variation in the vicinity of the fcc→sc phase transition, orientational glass-formation temperature $T_g = 90–100$ K, and other points on the temperature scale at which anomalies in physical properties have been observed also acquire a considerable significance.

Intense studies of the mechanical properties of fullerite C₆₀ are being carried out at present by several groups. Static or dynamic indentation technique are used for mechanical

TABLE I. Values of melting temperature T_m , elastic moduli μ and E , relative microhardness H_V/μ and H_V/E for fullerite C_{60} and materials with other types of bonds in the lattice.

Substance	T_m , K	T/T_m	μ		E		
			GPa		$10^3 H_V/\mu$	$10^3 H_V/E$	
C_{60}	1400*	0.08			28.4	32	12.3
	[14]	0.21			20[22]	26	10
Graphite	3770	0.08	20			50	20
	[15]		[17]				
CH_4	90.7	0.22	1.1			3.45	1.3
	[16]		[18]				
Ar	83.8	0.12	1.56			2.37	0.9
	[16]		[19]				
Kr	115.8	0.086	1.83			1.64	0.6
	[16]		[19]				
NH_3	196	0.39	3.04			40.5	15.6
	[16]		[20]				
NaCl	1073	0.27	15.5		38.7	7.3	2.8
	[15]		[21]		[21]		
Au	1336	0.22	27		78	8.3	3.2
	[15]		[15]		[15]		

*The estimate is based on the method of nonsymmetrized self-consistent field;¹⁴ T/T_m is the temperature of measuring the microhardness reduced to the melting point of the material: we assume that the moduli E and μ are connected through the relation $\mu = E/2(1 + \nu)$, in which the Poisson coefficient $\nu = 0.3$. The microhardness measurements were made on CH_4 ,²³ Ar,²⁴ Kr,²⁵ NH_3 ,²⁶ graphite,^{9,10} Au,²⁷ and NaCl (this publication).

testing in most cases because of the small size of the crystals being grown. The first and only stress-strain curve obtained as a result of compression of a sample with a cross section $\sim 0.5 \text{ mm}^2$ at a constant strain rate is given in Refs. 9 and 10.

Weak van der Waals interactions between molecules are responsible for low values of Vickers microhardness H_V and the yield stress σ_0 for fullerite C_{60} crystals. At room temperature, the typical value of $H_V \approx 0.2 \text{ GPa}$,⁸⁻¹² while the ratio $H_V/\sigma_0 \approx 20$.^{9,10,13} As regards microhardness, fullerite C_{60} crystals are comparable to graphite, plastic fcc metals of the gold type, or NaCl crystals. Table I gives a more detailed information on fullerite hardness as compared to other crystals. It can be seen that for comparable values of homologous temperature, the relative microhardness of fullerite is higher than the hardness of typical molecular crystals (except ammonium in which the ordered $P2_13$ structure is preserved up to the melting point), fcc metallic and alkali-halide crystals. The high relative hardness of ammonium and fullerite C_{60} in this series of molecular crystals is obviously due to much larger contribution of the noncentral component of forces to the molecular interaction, leading to the formation of an ordered sc phase of C_{60} below the phase-transition temperature.

The physical and mechanical properties of C_{60} crystals depend significantly on the past history of the samples: the purity of the initial raw material, the method of obtaining (either from solution or from the gaseous phase), the time of holding in the gaseous medium and its composition, and illumination. The crystals grown from the gaseous phase are distinguished by higher purity and structural perfection. At present, high-quality crystals with a mass up to 14 mg (and

volume up to 8.5 mm^3),²⁸ as well as larger crystals with the size $5 \times 3 \times 3 \text{ mm}$,²⁹ which are suitable for various investigations, can be obtained.

The most interesting effects observed in microplasticity investigations for fullerite C_{60} are associated with low-temperature structural transformations in this crystal. However, x-ray diffraction³⁰ and acoustic studies³¹ proved that the nature of phase transitions is determined to a considerable extent by various defects in real C_{60} crystals, such as the inclusions of C_{70} , amorphous phase, and other impurities inherited during the crystal growth or transformed as a result of thermal treatment. This is mainly manifested in the broadening of the temperature interval of orientational transition and its displacement toward lower temperatures, as well as in a considerable variation of temperature dependences of structural and thermodynamic parameters of C_{60} in the transition region.^{30,31} First measurements of the temperature dependence of microhardness of C_{60} (Refs. 8-10 and 12) have also revealed qualitative difference for samples synthesized in different ways. It was found that the value of H_V for polycrystalline samples grown from solution and containing impurities of C_{70} and other phases increases monotonically without noticeable anomalies as the temperature decreases from 600 to 81 K.^{10,32} More perfect crystals grown from the gaseous phase clearly manifest the fcc \rightarrow sc phase transition at $T_c \approx 260 \text{ K}$,¹⁻³ while the microhardness of such single crystals displays a discontinuity in the region of T_c (Refs. 8 and 12) and a noticeable kink at $T_0 \approx 155 \text{ K}$, which correlates with a weak anomaly on the temperature dependence of the lattice parameter.¹² Above T_c , the hardness of these crystals is virtually constant in the temperature range 260-300 K.^{8,10,12} At high temperatures $T > 370 \text{ K}$, an anomalous growth of the value of H_V with increasing temperature is observed.⁸

Considerable influence of the surrounding medium on the mechanical properties of fullerite C_{60} was noted in Refs. 9, 10, and 32 and investigated partially by the nanoindentation technique in Ref. 33. It was shown that the strain-hardening was the strongest when the crystals were held in argon or oxygen due to implantation of Ar atoms or O_2 molecules in octahedral voids in the fcc lattice of C_{60} .³³ For example, the microhardness and the Young modulus of a crystal placed in Ar atmosphere after 45 h of holding at room temperature increased by a factor of ~ 100 . Subsequent annealing led to restoration of the initial characteristics.

Finally, another important phenomenon was observed:³³ a change in microhardness as a result of irradiation of a C_{60} crystal with green light ($\lambda = 514 \text{ nm}$). The magnitude and sign of the effect were determined by the gaseous medium: the crystal was strain-hardened in oxygen atmosphere, while in argon its hardness decreased. This peculiar photoplastic effect is associated with the formation of apex C- O_2 bonds upon the implantation of oxygen molecules in the crystal and with the polymerization of C_{60} molecules in the chains in the argon atmosphere. This effect differs from the photoplastic effects studied comprehensively for semiconducting crystals^{34,35} and in irradiated alkali-halide crystals³⁶ and obviously requires further investigations.

Chemical and thermal etching of the crystal surface in

the vicinity of the indentation revealed that the plastic deformation of fullerite C_{60} crystals is of dislocation origin.^{37,38} This means that the peculiarities of the temperature dependence of H_V must be attributed to a change in the mobility of dislocations: the high-temperature anomaly can be due to the interaction of dislocations with impurity molecules that diffuse in the crystal,⁸ while the enhancement of the $H_V(T)$ dependence in the sc phase below 155 K is associated with the relaxation of orientational ordering of C_{60} molecules in the elastic field of moving dislocations.¹³ However, the slip crystallography as well as the structure of dislocations in these crystals have been studied incompletely.

This research is devoted to (1) a more detailed description of the results of studies of the temperature dependence of the lattice parameters and microplasticity of pure C_{60} crystal, which were briefly discussed in Ref. 12, (2) an analysis of slip crystallography in the fcc and sc phases, (3) the study of microhardness anisotropy, and (4) an analysis of the effect of crystal annealing on the microhardness anomaly in the region of the fcc→sc transition.

2. MATERIAL AND EXPERIMENTAL TECHNIQUE

The samples were obtained from commercial fullerite having a purity of ~99.5% by double sublimation in Ar. The initial material was placed in a quartz boat of the sublimation column; argon was blown under a pressure of ~1 atm in the direction of temperature growth; C_{60} was heated approximately to 920 K during several hours; sublimated fullerite was returned to the column, and the process was repeated. According to the results of high-sensitivity liquid-phase chromatography, the purity of the obtained fullerite was higher than 99.9%. In addition to fine-disperse fraction with a grain size 10^{-1} – 10^{-2} mm, the powder contained isolated crystals of size $\sim 2 \times 1 \times 0.3$ mm. Some of the crystals had a larger plane parallel to the $\{111\}$ direction, some others were of the $\{100\}$ type, while the edges, as a rule, had an orientation $\langle 110 \rangle$. Because of the uncontrollable growth, the faceting of individual crystals deviated from the crystallographic direction. Islets with specular surfaces of the $\{111\}$ or $\{100\}$ type, which are convenient for slip crystallography, were observed at the faces of the crystals.

The morphology of the surface of initial and indented samples was studied with the help of an optical microscope. The microhardness measuring technique in the temperature range 81–300 K was described in Ref. 39. All experiments were made in atmosphere, nitrogen vapor, and in liquid air ($T=81$ K) on the samples not protected from natural illumination. The spread in data was reduced by multiple measurements on the same sample. A thin layer of the surface being indented was removed between measurements by sample polishing with chamois leather impregnated with benzene. The relative error in determining the average value of microhardness did not exceed 2%. Here we present the average values of microhardness calculated from the results of measurements of 10–20 indentations.

In the case of x-ray diffraction studies, the coarse-grain sublimated powder was crushed and annealed in vacuum for 1 h at 500 K. Such a procedure of annealing made it possible to obtain samples free of macrostresses with a crystallite size

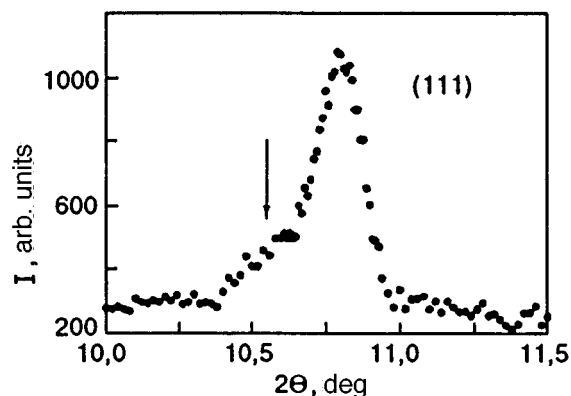


FIG. 1. The profile of the (111) x-ray reflection of fullerite C_{60} at room temperature. The arrow indicates the position of pseudo-Bragg diffraction.

10^{-4} – 10^{-5} mm. Sample homogeneity and quality were monitored from the profile and width of diffraction reflexes. In the course of measurements, the samples were permanently in vacuum and were protected from illumination. Structural studies were carried out in $Cu-K_{\alpha}$ radiation on an automated DRON-type diffractometer in the temperature range 30–293 K by using an original liquid-helium cryostat.⁴⁰ The sample temperature was measured with a platinum resistance thermometer. The error in temperature stabilization was ± 0.05 K, and the error in determining the lattice parameters did not exceed ± 0.001 Å. The errors in determining the linewidth and intensity for x-ray reflexes are presented in the figures.

3. DISCUSSION OF RESULTS

3.1. X-ray studies

An analysis of x-ray diffraction pattern obtained at room temperature has proved that the process of dispersion and subsequent annealing did not lead to contamination of the sublimated material with any impurities. X-ray diffraction patterns contained only reflections from the cubic fcc phase of fullerite C_{60} . The value of the lattice parameter $a = 14.161$ Å averaged over several measurements is in good agreement with the data for single crystals.^{11,41,42} However, diffraction for the crushed material was characterized by an enhanced general background and by the emergence of additional pseudo-Bragg diffraction in the form of asymmetry or an “arm” in the (111) reflection profile (Fig. 1). The latter can be due to violation of the stacking order in atomic layers (111) of the fcc lattice, which lower the symmetry of defective regions of the crystal to the hexagonal symmetry. The effect of various types of stacking faults on the diffraction pattern for fullerite C_{60} crystals is considered in detail by Vaughan *et al.*⁴³ Such structural inhomogeneities in fullerite crystals can lead to a number of anomalies in the physical properties in the region of orientational phase transition: the formation of the second heat-capacity peak⁴³ and to a noticeable “blurring” of this transition detected by x-ray diffraction technique (see below).

X-ray studies in the temperature range 30–293 K confirmed, in general, the existing concepts concerning struc-

TABLE II. Angles and experimental values of intensities of x-ray reflections in fullerite C₆₀ at 32 K.

No.	$2\Theta_{\text{exp}}^{\circ}$	I_{exp}	hkl	$2\Theta_{\text{calc}}^{\circ}$	$\Delta(2\Theta^{\circ})$
			100	6.360	
			110	9.000	
1	11.03	1000	111	11.028	-0.002
			200	12.741	
			210	14.252	
			211	15.621	
2	18.07	925	220	18.056	-0.014
			300	19.161	
			310	20.208	
3	21.21	720	311	21.206	-0.004
4	22.17	200	222	22.161	-0.009
			320	23.078	
			330	27.228	
5	28.02	60	331	27.989	-0.031
6	28.76	75	420	28.731	-0.029
			421	29.456	
			332	30.166	
7	31.53	86	422	31.541	0.011
			430	32.210	
			510	32.865	
8	33.53	76	511	33.510	-0.020
			520	34.767	
			600	38.886	
9	39.48	52	610	39.445	-0.035
			611	39.997	
			620	41.082	
10	41.56	32	540	41.616	0.056
11	42.19	23	541	42.144	-0.046
12	42.65	25	533	42.667	0.017
13	43.21	390	622	43.185	-0.025
			630	43.698	
			444	45.209	
14	45.74	58	632	45.704	-0.036
15	46.17*	35	550	46.195	0.025
16	46.71	95	551	46.681	-0.029
			640	47.164	
			722	49.524	
17	49.93*	74	730	49.987	0.064
18	50.46	280	731	50.446	-0.014
			650	51.355	
			820	54.451	
19	54.86	60	821	54.883	0.023
			653	55.313	
			664	62.723	
20	63.17	29	850	63.120	-0.05
21	63.47*	34	930	63.514	0.044
			931	63.908	
			961	74.121	
22	74.82	57	1042	74.852	0.032
			1100	75.218	

*Structural reflections which belong to a space symmetry group lower than $Pa\bar{3}$.

tural transformation occurring during the cooling of C₆₀ crystals. The fcc→sc phase transition is accompanied by the emergence of superstructural reflexes on diffraction patterns, corresponding to a decrease in the total symmetry of the crystal as a result of orientational ordering of molecules. Most of the observed superstructural reflexes are identified in the space group $Pa\bar{3}$. A part of experimental diffraction pattern at $T=32$ K is presented in Table II, together with the theoretically calculated reflexes for the lattice parameter $a=14.043$ Å. In addition to the experimental ($2\Theta_{\text{exp}}^{\circ}$) and theoretical ($2\Theta_{\text{calc}}^{\circ}$) values of the reflection (hkl) angles,

Table II also contains the experimental values of the intensities (I_{exp}) of the observed reflections in relative units, normalized to the intensity of the strongest reflections (111). The first column of Table II contains the number of observed reflections, while the last column shows the difference $\Delta(2\Theta^{\circ})$ between the theoretical and experimental diffraction angles. For large diffraction angles, several superstructural reflections of the ($hk0$) type with odd h and k (marked by asterisks in Table II), which do not belong to $Pa\bar{3}$ symmetry and whose intensity is comparable with that of the main structural reflections in this range of diffraction angles,

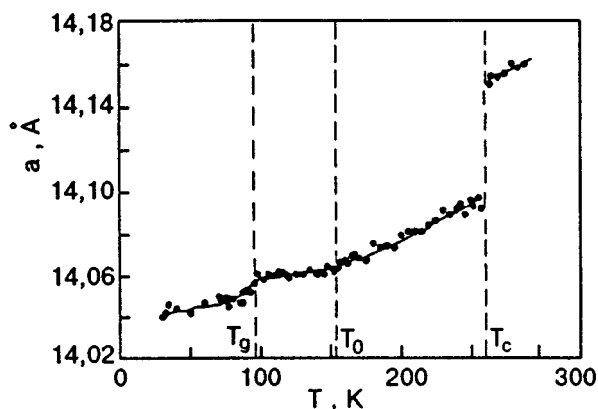


FIG. 2. Temperature dependence of the lattice parameter for the fullerite C_{60} : T_c is the temperature of orientational phase transition $fcc \rightarrow sc$, T_0 and T_g are the temperatures corresponding to the beginning and end of the formation of the orientational glass, respectively.

are observed. Since powder samples contained a large number of regions with stacking faults with a symmetry lower than that of fcc , it can be naturally assumed that the orientationally ordered structure has a symmetry lower than $Pa3$ in these regions also. This circumstance can be responsible for the emergence of additional superstructural reflections at $T < T_c$. It should be noted that the intensity of such reflections must increase with the volume of defective regions. However, we could not verify much an increase.

The temperature dependence of the lattice parameter a (Fig. 2) contains regions corresponding to three characteristic temperatures. The $fcc \rightarrow sc$ phase transition is accompanied by a jump in the lattice parameter whose relative decrease ($\Delta a/a \approx 0.33\%$) as a result of the transition is in good agreement with the results obtained in Refs. 2 and 42. The temperature variation of the lattice parameter in the high-temperature phase corresponds to the available experimental data.^{2,5,41,42} The obtained phase-transition temperature $T_c = 260$ K which we obtained virtually coincides with the temperature typical of single-crystal samples.^{2,11} Detailed analysis of x-ray patterns revealed the coexistence of the fcc and sc phases in the vicinity of the phase transition temperature $T_c \pm 3$ K. The presence of two phases in such a significant temperature interval during an orientational phase transition is apparently due to dispersion in the values of phase-transition temperature in defective regions of the crystal. The regions of short-range orientational order in the parts of the crystal with stacking disorder near T_c is characterized by a smaller correlation radius of the orientational interaction as compared to the rest of the crystal,⁴³ and hence by a lower phase-transition temperature T_c . According to the results on inelastic x-ray and neutron scattering,⁴⁴ the regions of short-range orientational order in perfect C_{60} single crystal in which translational disorder of the stacking fault type is not observed have a correlation length of the order of 40 \AA (at $T = 265$ K).

At $T_g \approx 95$ K, the $a(T)$ dependence has a clearly manifested kink (see Fig. 2); this anomaly is also well known from previous structural studies.^{2,12} The peculiarity in the behavior of $a(T)$, which is observed at $T_0 = 155$ K and about

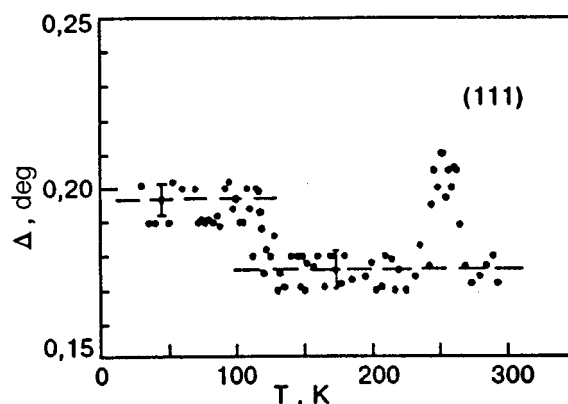


FIG. 3. Temperature dependence of the half-width Δ of (111) x-ray reflection.

which the information is controversial,^{2,6} was detected by us more clearly. It should be noted that some other parameters of fullerite have certain peculiarities just in the vicinity of this temperature (this problem was discussed, for example, in the review in Ref. 6).

The peculiarities on the temperature dependence of some physical parameters at $T < 160$ K are associated by David *et al.*^{2,4} with the retardation of rotation of C_{60} molecules about $\langle 111 \rangle$ axes, which is manifested in an increase in the lifetime of orientational defects (hexagonal configurations of pairs of neighboring molecules) upon a decrease in temperature. Subsequent cooling leads to virtually complete freezing of the rotational motion and to the formation of orientational glass at $T < 95$ K (with a fixed relation between pentagonal and hexagonal configurations of C_{60} molecules). This explains the increase in the half-width of x-ray reflections in the region $T_g < T < T_0 \approx 155$ K observed in our experiments. The results of measurement of the half-width Δ of the profile of one of the main reflections (which are structural in the case of an fcc lattice) are presented in Fig. 3. As the temperature decreases from 155 K to the glass-transition point, the half-width of the reflection profile undergoes an overall variation of 10–12%. A similar diffraction involving the variation of the reflection profile half-width was observed earlier in solid solutions of simple molecular crystal N_2 –Ar⁴⁵ and O_2 –Ar⁴⁶ during the formation of orientational glass in them. However, the glass-formation process in these systems was accompanied by a more significant broadening of reflections (by more than 70%). We believe that the freezing of molecules in random orientations leads to their non-uniform static displacements from lattice sites. The magnitude of displacements, and hence the broadening of diffraction reflections, are determined by the contribution of anisotropic forces to the lattice energy. In contrast to this effect, the noticeable increase in the profile half-width of the (111) reflection near T_c (Fig. 3) is due to the superposition of reflections from two coexisting phases with a small difference in molecular volumes, while the shape of the temperature dependence of the half-width of the (111) reflection in the two-phase region characterizes the change in the concentration of phases upon a transition through T_c .

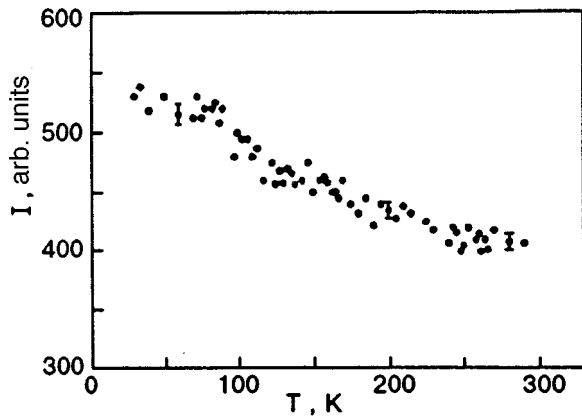


FIG. 4. Temperature dependences of the intensity of (111) x-ray reflections.

We have not discovered any anomalies on the temperature dependences of the intensity of structural reflections in the entire temperature range of investigation. As the temperature decreases, their intensity increases monotonically (Fig. 4) mainly due to a change in the Debye–Waller factor as a result of the decrease in the amplitude of mean-square displacements of the molecules. A decrease in temperature below T_g leads to an anomalous retardation of the growth of intensity $I(T)$ (see Fig. 4). Since the peculiarities on the temperature dependences of the physical properties of fullerenes are mainly determined by the behavior of its orientational subsystem, it would be interesting to study the temperature dependence of the intensity of superstructural reflections. Superstructural reflections typical of the $Pa3$ lattice were studied in detail for C_{60} single crystals.^{43,47–49} The results described in these publications show that a retardation of the growth of $I(T)$ similar to that shown in Fig. 4 is typical of most of superstructural $Pa3$ reflections upon a transition to a glass-like phase.

3.2. Growth twins and slip crystallography

The polished surface of crystals displayed plane-parallel stripes aligned along the $\langle 110 \rangle$ directions, which were preserved after multiple polishing. One of such stripes observed on the $\{100\}$ plane is shown in Fig. 5. Such stripes are apparently growth twins corresponding to $\{111\}\langle 112 \rangle$ systems typical of fcc crystals. They become visible because of selective etching of twinned planes and their boundaries under the action of benzene. Growth twins are typical defects in

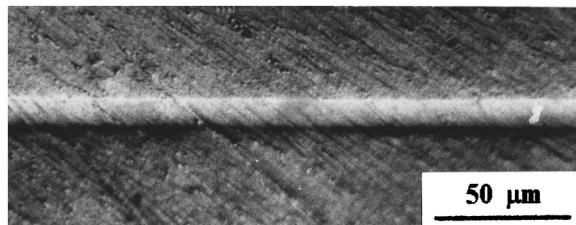


FIG. 5. The growth twin detected on the $\{100\}$ plane of the C_{60} crystal as a result of its mechanical and chemical polishing with chamois leather impregnated with benzene. The direction of twin boundaries coincides with the $\langle 110 \rangle$ direction.

fullerite C_{60} crystals.²⁹ The width of the twins varied from 5–10 μm to tens of micrometers. The effect of growth twins on microhardness was not studied, but it would hardly be significant for a low density of twin boundaries. However, twins do play a noticeable role in the formation of cracks. Indentation in the vicinity of twin boundaries always leads to the formation of cracks along the latter. We did not observe the formation of deformation-induced twins under the action of a concentrated force, but it cannot be ruled out that strongly distorted regions of the crystal can contain a large number of deformation-induced stacking faults in the vicinity of indentations.

The cubic lattice of fullerite C_{60} as well as the familiar habitus of the crystals make it possible to determine unambiguously the slip systems in the high- and low-temperature phases from an analysis of the pattern of slip traces in deformed regions in the region of indentation (Fig. 6). It is well known that a slight slippage in fcc crystals can easily be realized along the octahedral system $\{111\}\langle 110 \rangle$. For crystals with a sc lattice, the systems $\{100\}\langle 100 \rangle$ or $\{110\}\langle 100 \rangle$ might turn out to be advantageous from the energy point of view.⁸ Proceeding from these considerations, let us compare the pattern of slippage stripes on the sample surface with the directions of traces of crystallographic planes $\{111\}$, $\{100\}$, and $\{110\}$ on the habitus planes (111) and (100) of the crystal.

Clearly manifested slippage planes were formed in the vicinity of an indentation for loads exceeding 0.1–0.2 N. The stripes formed on the (111) plane under a loading of 0.2 N ($T=290$ K) can be seen in Figs. 6a and 6b (at $T < T_c$, the pattern is similar). Repeated indentation under the same load (Fig. 6b) only led to a more intense slippage and elongation of the stripes formed as a result of the previous indentation. Figure 6d shows that the traces of the three types of the planes $\{111\}$, $\{100\}$, and $\{110\}$ on the (111) plane of the sample have the same $\langle 110 \rangle$ direction. Planes of the $\{110\}$ type can have the $\langle 112 \rangle$ direction also. These two sets of traces can be identified only if the crystallographic direction of at least one of the crystal edges is known. The triangles of traces turned relative to one another reflect converging and diverging slip systems along which the transfer of matter is accomplished in the vicinity of the indenter to the surface of the sample and to its bulk. This explains different (black and white) contrasts of parallel slippage stripes in Figs. 6a and 6b. In the case of the $\{110\}\langle 100 \rangle$ system, the traces in the $\langle 112 \rangle$ direction correspond to the three slippage planes $(0\bar{1}1)$, $(1\bar{1}0)$, and $(\bar{1}01)$ from the $\{110\}$ family, which intersect the (111) surface of the sample at right angles. Naturally, an analysis of the plastic shear pattern (slip steps) on the $\{111\}$ plane alone³⁸ does not lead to an unambiguous conclusion about slip crystallography (especially at temperatures below the phase-transition point).

Figure 6c shows the microscopic structure of the deformed region of the sample indented at $T=81$ K at the surface that deviates slightly from the (100) plane. It can be seen from Fig. 6e that the pattern of the traces of the $\{111\}$, $\{100\}$, and $\{110\}$ planes intersecting the (100) plane is extremely simple. Remarkably, only the slippage planes of the $\{111\}\langle 110 \rangle$ can be either converging or diverging, form-

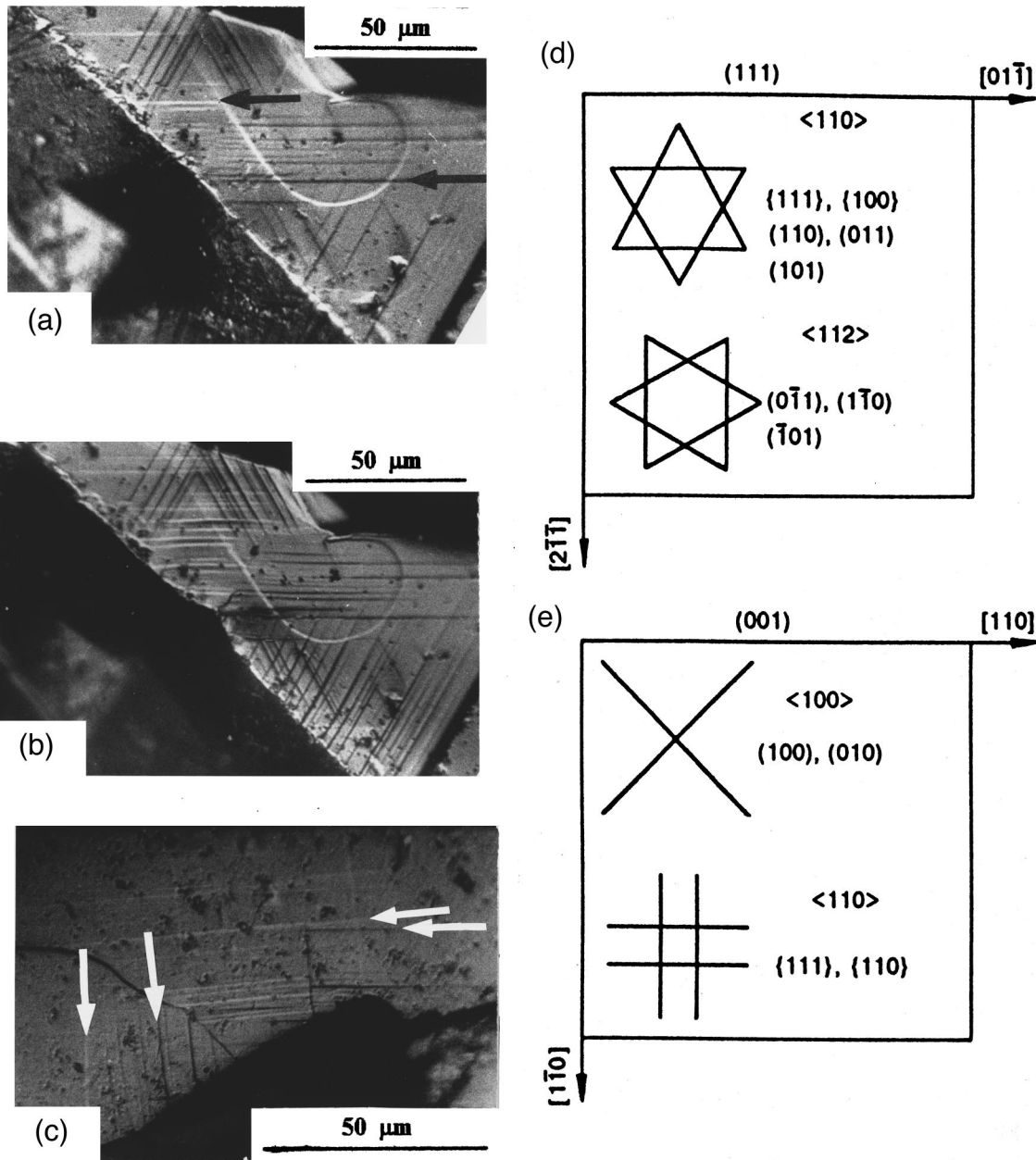


FIG. 6. Slip stripes bear the impression of the indenter on the (111) (a,b) and (100) (c) planes and schematic diagrams of possible slip planes $\langle 111 \rangle$, $\langle 100 \rangle$, and $\langle 110 \rangle$ on habitus planes of the C_{60} crystal: the first and repeated indentation at $P=0.2$ N and $T=290$ K(a,b); and indentation at $P=0.35$ N and $T=81$ K(c); the (111) plane, the direction of traces $\langle 110 \rangle$ and $\langle 112 \rangle$ (d), the (001) plane, the direction of traces $\langle 100 \rangle$ and $\langle 110 \rangle$ (e).

ing parallel traces on the (100) plane. The $\{110\}\langle 100 \rangle$ system with the Burgers vector lying in the $\{100\}$ plane naturally is not seen. A deviation of the sample surface from (100) leads to the emergence of nonparallel traces (Fig. 6c). Different optical contrasts of steps on the surface and their nonparallelism indicate that the pairs of slippage planes marked by arrows and forming small angles with one another belong to different families $\{111\}\langle 100 \rangle$.

Thus, our microstructural observations of slippage stripes and their geometrical analysis lead to the unambiguous conclusion that only the octahedral slip system $\{111\}\langle 110 \rangle$ is active at temperatures in the interval 81–300 K.

Although such a conclusion was made earlier in Refs. 12 and 38, crystals of two orientations were used only in Ref. 12 and in the present work for its verification.

The conservation of slip in $\{111\}$ -type planes during fcc \rightarrow sc phase transition is a phenomenon that has been studied well in ordered alloys Cu_3Au and Ni_3Mn .⁵⁰ It is possible that like in these alloys, slip in $\{111\}$ planes in the ordered sc-phase of C_{60} occurs through the motion of partial dislocations accompanied with the formation of low-energy out-of-phase boundaries.¹² The microscopic nature of conservation of slip systems in C_{60} crystals upon a fcc \rightarrow sc transition is undoubtedly interesting and deserves further investigations.

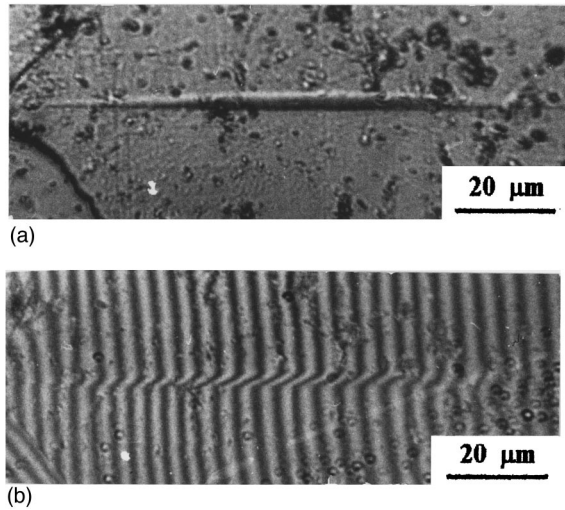


FIG. 7. Lens-shaped shear region formed as a result of indentation of the (100) plane in the C_{60} crystal at $T=290$ K and $P=0.7$ N: metallographic microscope (a) and interference microscope (b).

3.3. Localization of slip

The deformation of C_{60} crystals by indentation is characterized by noticeable localization of plastic shear strains leading to the formation of clearly manifested steps upon the emergence of a slip stripe at the surface (Fig. 7a,b). A lens-shaped shear region is formed as a result of indentation under a large load applied to the indenter. It resembles a twin in shape, but the height of a step at the surface turns out to be smaller than in the case of a twin in the fcc lattice by a factor of 2.5. The lens-like shape is due to deceleration of a slip strip at cracks restricting its elongation on both sides.

It is well known that slip localization upon indentation is enhanced upon an increase in rigidity of the crystal, for example, as a result of doping, irradiation, or cooling.⁵¹ This phenomenon should not be typical of pure molecular crystals (at least in their high-temperature phase).⁷ The C_{60} crystals investigated by us were initially saturated with Ar atoms which, according to Haluska *et al.*,³³ can lead to a significant strain-hardening and a decrease in plasticity even in an orientationally disordered state.

3.4. Microhardness of C_{60} crystals

Dependence of H_V on the load applied to the indenter. The dependences of the square $(2a)^2$ of the impression diagonal on load P , obtained on (100) plane at 81 and 290 K, are shown in Fig. 8. The linear relation between $(2a)^2$ and P corresponding to the constancy of $H_V(P)$ was observed only for loads $P \leq 0.1$ N at 290 K and $P \leq 0.075$ N at 81 K. At higher loads on the indenter, the material was broken. Cracks in the vicinity of impression had no clearly manifested crystallographic direction like in the case of brittle crystals, but the $\langle 110 \rangle$ direction can be indicated as a preferred direction of their propagation. At nitrogen temperatures, crack formation was more intense (see the inset in Fig. 8) and started at lower loads.

The absence of the $H_V(P)$ dependence for the $\{111\}$ plane was observed in Ref. 8 at room temperature for load-

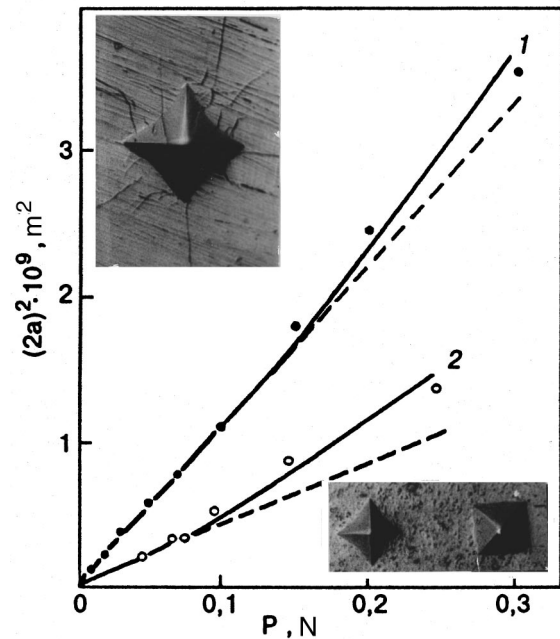


FIG. 8. Dependence of the square of the impression of the indenter on the (100) plane of the C_{60} crystal on the load applied to the indenter at $T=290$ K (curve 1) and $T=81$ K (curve 2). The upper inset shows the impression of the indenter on the (100) plane at $P=0.25$ N and $T=81$ K. The diagonal of the impression is directed along $[011]$. The lower inset shows the impressions of the indenter in the (100) plane for $P=0.05$ N and $T=290$ K; the horizontal direction is parallel to $[110]$.

ings down to ~ 0.14 N, while in Ref. 28 the microhardness for the same plane decreased significantly upon an increase in load to ~ 0.2 N and only after that it remained unchanged up to $P=0.8$ N. The existence of a wide range of loads for which $H_V(P) = \text{const}$ obviously indicates the homogeneity of the crystals under investigation due to favorable conditions of their growth. The reason behind a decrease in microhardness and increasing load (impression depth) observed in Refs. 9 and 10 could be the concentration gradient of impurities diffusing through the sample surface.

Microhardness anisotropy. The anisotropy of plastic slip is manifested in experiments on microindentation of C_{60} crystals in experiments on microhardness first in different values of microhardness for different indentation planes for the same values of P and T , and second, in a dependence of the impression shape on the direction of the indenter diagonal. It can be seen from Fig. 8 that the impressions are concave if the indenter diagonal is oriented along the $\langle 110 \rangle$ direction and convex if the diagonal is oriented along $\langle 100 \rangle$. This is due to the displacement of the material ejected during the intrusion of the indenter in the slip direction as for other cubic crystals⁵¹ (in the case of fullerite C_{60} , this is the $\langle 110 \rangle$ direction; see the schematic diagram in Fig. 6e). It should be noted that the preservation of the shape of the impression upon a change in temperature of indentation is an indication of preservation of the slip system in C_{60} during the phase transition.

At all temperatures, the value of microhardness measured in the (111) plane was higher than that measured in the (100) plane (Fig. 9). The ratio of the values of H_V for these

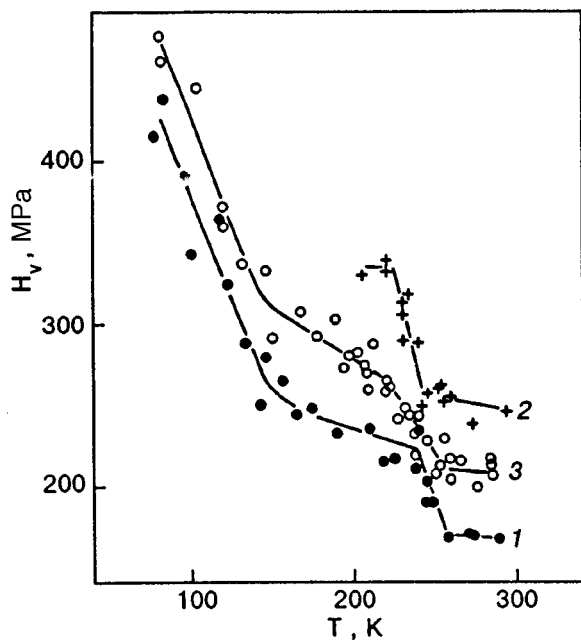


FIG. 9. Temperature dependences of microhardness obtained as a result of indentation of habitus planes (100) (curve 1) and (111) (curves 2 and 3) for three different C_{60} crystals.

planes is ~ 1.25 – 1.5 in the region of room temperatures, which is in good agreement with the results obtained in Ref. 11; as the temperature decreases, this ratio becomes smaller and attains the value ~ 1.1 at 81 K. The anisotropy of hardness is probably due to different values of strain hardening of the material under the indenter, whose intensity can depend on the direction of indentation $\langle 111 \rangle$ or $\langle 110 \rangle$ (see the schematic diagram in Figs. 6d and 6e).

Temperature dependence of microhardness. In order to analyze the temperature dependence of microhardness, we used a load ~ 0.05 N, which ensures the satisfaction of the condition $H_V(P) = \text{const}$ in the entire temperature interval of interest.

Figure 9 shows three $H_V(T)$ dependences obtained as a result of indentation of the (100) plane (curve 1)¹² and the (111) plane (curves 2 and 3). The absolute values of microhardness at room temperature ($H_V^{100} = 170$ MPa and $H_V^{111} = 210$ – 250 MPa) are close to those obtained by other authors.^{8,10,11,28} The spread in the values of H_V for different samples of the crystals with the same orientation was $\sim 20\%$. The same spread was also observed in Ref. 8.

The main peculiarities of the temperature dependence of microhardness can be reproduced for all the samples, are insensitive to the orientation of the indentation plane, and are obviously associated with specific structure of fullerite.^{8,12,13} The first of these peculiarities is the athermal nature of H_V in the high-temperature phase of C_{60} even when impurity diffusion processes leading to the fixation of dislocations are included.⁸ This feature is typical of the mechanical properties of high-symmetry crystals and can indicate that the fcc fullerite belongs to plastic molecular crystals.⁷

Two anomalies (namely, the step-wise variation of microhardness in the region of the fcc \rightarrow sc transition and the kink on the $H_V(T)$ dependence in the region of $T \sim 155$ K,

correlate with the observed anomalies on the temperature dependence of the lattice parameter (see Fig. 2). Note that an increase in microhardness in the sc phase can be partly due to an increase in the elastic moduli for fullerite: the increase in Young's modulus during a phase transition is $\sim 8\%$, while the cooling from room temperature to 6 K causes its increase by 40%.²² At the same time, the step on H_V in the transition region amounts to 30–50%,^{8,12} while the microhardness increases approximately by a factor of two in the temperature range 290–81 K. The main contribution to the increment of H_V during cooling is undoubtedly associated with a considerable effect of thermally activated processes on the slip kinetics (mobility of dislocations). Among other things, an increase in the size of the deformation region with well-developed slip stripes upon an increase in the holding time under loading indicates the activation nature of slip evolution (Fig. 6b).

Two types of relaxation processes occurring in the elastic field of a dislocation moving in the sc phase of fullerite C_{60} were analyzed in Ref. 13. It was shown that these processes are due to dynamic interaction of dislocations with rotational degrees of freedom of C_{60} molecules. Each such process can make a significant contribution to dislocation drag. In the immediate vicinity of T_c , the dominant role is played by the relaxation losses accompanying the interaction of the elastic field of dislocations with the field of the order parameter which corresponds to this transition. According to the estimates obtained in Ref. 13, the proposed mechanism can explain the stepwise increase in H_V below T_c . In the temperature range of ~ 160 K, the main role is played by dynamic losses of the dislocation, which are associated with the thermally activated relaxation in the system of pentagonal and hexagonal molecular configurations, whose equilibrium is violated by the elastic dislocation field. This drag mechanism can be used to explain the beginning of a significant increase in H_V upon a decrease in temperature in the region of orientational vitrification of fullerite.

It should be observed that the relaxation of the order parameter as well as the activation transitions in the system of pentagonal and hexagonal configurations affect the acoustic properties of the fullerite C_{60} quite significantly. Hence the acoustic anomalies must be closely related physically to the $H_V(T)$ anomalies below T_c .¹³

Effect of impurities on the microhardness anomaly in the fcc \rightarrow sc transition region. The stepwise increase in microhardness associated with the phase transition occurs over a fairly wide temperature interval between 10 K (Refs. 8 and 12) and 20 K or more (Figs. 9 and 10). The $H_V(T)$ dependences obtained during cooling and heating of the sample are identical to within the measuring error. It is known from structural,^{30,52,53} acoustic^{31,54,55} and NMR studies,^{56,57} as well as the data on heat capacity^{58,59} that the width of the phase transition ΔT and the behavior of thermodynamic properties of fullerites in the vicinity of T_c depend significantly on the presence of impurities in the sample. A significant concentration of the interstitial impurities of the C_n -type molecular fragments, N_2 or O_2 molecular components or other components of air may not only lower the superconducting transi-

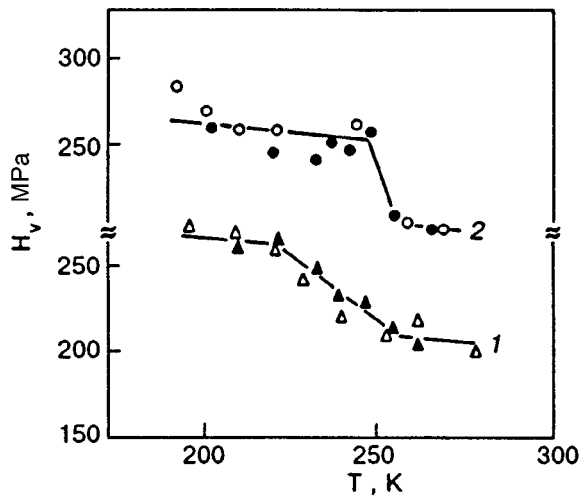


FIG. 10. Temperature dependences of microhardness in the region of the fcc→sc transition obtained on the same C_{60} crystal subjected to different treatment: the initial crystal polished before the measuring microhardness (curve 1, light triangles), the same crystal polished after annealing in vacuum (the annealing mode is given below) and holding in air for five days (dark triangles); the crystal polished and annealed in a 10^{-3} Torr vacuum for 24 h at 400 K (curve 2; the symbols \circ and \bullet correspond to different experiments).

tion temperature T_c , but also considerably increase the interval ΔT (up to ~ 10 K or more).³⁰

The extended step on the $H_V(T)$ dependence during a transition through T_c may also be due to the molecular impurities trapped by the sample surface from the surrounding air or during mechanical and chemical polishing. In order to verify this assumption, we annealed a sample in a vacuum of 10^{-3} Torr at 400 K for 24 h. Figure 10 shows that annealing leads to an abrupt narrowing of the temperature interval of variation of microhardness.

In our opinion, atmospheric oxygen is the most probable trapped impurity. In contrast to noble gases, oxygen molecules affect significantly the intermolecular forces in fullerite²⁸ and determine the peculiarities of the fcc→sc phase transition to a certain extent.^{60,61} The high mobility of oxygen in C_{60} , which is due to a low diffusion activation energy of 0.24 eV,⁶² is a factor facilitating the saturation of the surface layers of the sample with oxygen as well as their purification in a moderate vacuum at a low temperature ($T \sim 400$ K). The details of the effect of impurities on the phase transition in C_{60} require further investigations.

CONCLUSIONS

1. The crystal structure, the lattice parameters, the half-width and intensity of x-ray reflections of fullerite C_{60} are studied by the method of x-ray diffractometry in the temperature range 30–293 K. It is shown that the temperature corresponding to the orientational phase transition in high-purity fullerite is $T_c = 260$ K and that it nearly coincides with the value typical of single crystals.

2. It is found that the samples under investigation contain a noticeable number of regions with stacking faults. A two-phase region with an interval of blurring of ± 3 K due to dispersion of the of transition temperatures in defective re-

gions of the crystal is detected in the fcc→sc transition. Along with superstructural reflections typical of $Pa3$ lattice, a number of $(hk0)$ reflections with odd h and k corresponding to a lower symmetry of the orientational ordering of molecules are observed in the low-temperature phase of fullerite. This symmetry can be realized in crystal regions with stacking faults.

3. The temperature dependence of the lattice parameter a manifests three distinct features: the jump $\Delta a/a = 3.3 \times 10^{-3}$ in the parameter at the phase-transition temperature T_c , weakening of the $a(T)$ dependence at $T_0 \leq 155$ K, and a kink at $T_g \approx 95$ K, which are associated with the beginning and termination of molecular orientation freezing. It is shown that the formation of orientational glass is accompanied by a considerable increase in the half-width of structural reflections. Anomalous deceleration of the increase in the intensity of structural reflections with decreasing temperature is observed in the region corresponding to orientational glass ($T < T_g$).

4. Microscopic observations of the surface and crystallographic analysis of the patterns of plastic shears in the (111) and (100) planes lead to the unambiguous conclusion concerning the activity of the only slip system of the $\{111\} \times \langle 110 \rangle$ type in the fcc and sc phases.

5. The temperature dependence of microhardness H_V of C_{60} crystals is studied in the temperature range 81–293 K. The hardness of the fcc phase normalized to the elastic modulus turns out to be higher than the hardness of typical molecular crystals at comparable homological temperature values. This fact as well as considerable localization of slippage indicates that the crystals studied in this research cannot be classified as plastic crystals in view of the presence of hardening impurities in them.

6. The microhardness increases stepwise by approximately 30% upon a transition through T_c , while at $T < 160$ K the $H_V(T)$ dependence becomes stronger. These anomalies are regarded as consequences of dislocation drag due to relaxation losses during the interaction of the elastic field of dislocations with the field of the orientational order parameter (the T_c region) and with the system of pentagonal and hexagonal configurations of C_{60} molecules whose equilibrium is violated by a moving dislocation (the region of $T \approx 160$ K).

7. The increase in the value of H_V during the fcc→sc transition is observed in the temperature interval larger than 10 K. The width of this interval decreases as a result of annealing in vacuum, which is apparently due to the purification of surface layers from gaseous impurities saturating the crystal during its storage in air.

8. Plastic deformation in C_{60} crystals is anisotropic, which is manifested, for example, in the dependence of the value of H_V on the direction of the indentation plane: $H_V^{111} \approx (1.25-1.5)H_V^{100}$ at $T = 293$ K.

This research was carried out under financial support of the Ukrainian State Committee on Science, Engineering, and Industrial Policy (project No. 09.01.01/033-92 "Material") and was supported in part, by the Soros International Science Foundation.

- ¹P. A. Heiney, J. A. Fischer, A. R. McGhie *et al.*, *Phys. Rev. Lett.* **66**, 2911 (1991).
- ²M. I. F. David, R. M. Ibberson, T. J. S. Dennis *et al.*, *Europhys. Lett.* **18**, 219 (1992).
- ³V. M. Loktev, *Fiz. Nizk. Temp.* **18**, 217 (1992) [*Sov. J. Low Temp. Phys.* **18**, 149 (1992)].
- ⁴W. I. F. David, R. M. Ibberson, and T. Matsuo, *Proc. Roy. Soc. London* **A442**, 129 (1993).
- ⁵J. E. Fischer and P. A. Heiney, *J. Phys. Chem.* **54**, 1725 (1993).
- ⁶J. D. Axe, S. C. Moss, and D. A. Neumann, in *Solid State Physics* (ed. by H. Ehrenreich and F. Spaepen), Acad. Press, New York (1994), vol. 48.
- ⁷J. Timmermans, *Phys. Chem. Sol.* **18**, 1 (1961).
- ⁸M. Tachibana, M. Michiyama, K. Kikuchi *et al.*, in *Crystal Growth of Organic Materials*, ACS Conference Proceedings Series (ed. by A. S. Myerson, D. A. Green, and P. Meenan), American Chemical Society (1996).
- ⁹Yu. A. Ossipyan, V. S. Bobrov, Yu. S. Grushko *et al.*, *Appl. Phys.* **A56**, 413 (1993).
- ¹⁰V. S. Bobrov, R. A. Dilanyan, L. S. Fomenko *et al.*, in *Solid State Phenomena 35–36* (ed. by J. Rabier, A. George, Y. Brechet, and L. Kubin) (1994).
- ¹¹J. Li, S. Komiya, T. Tamura *et al.*, *Physica* **C195**, 205 (1992).
- ¹²L. S. Fomenko, V. D. Natsik, S. V. Lubenets *et al.*, *Fiz. Nizk. Temp.* **21**, 465 (1995) [*Low Temp. Fiz.* **21**, 364 (1995)].
- ¹³V. D. Natsik, S. V. Lubenets, and L. S. Fomenko, *Fiz. Nizk. Temp.* **22**, 337 (1996) [*Low Temp. Fiz.* **22**, 264 (1996)].
- ¹⁴V. I. Zubov, N. P. Tretiakov, J. N. Teixeira Rabelo, and J. S. Sanches, *Phys. Lett.* **A194**, 223 (1994).
- ¹⁵J. Kay and T. Lebi, *Tables of Physical and Chemical Constants* [Russian transl.], Gos. Izd. Fiz. Mat. Lit., Moscow (1962).
- ¹⁶*Cryocrystals* [in Russian] (ed. by B. I. Verkin and A. F. Prikhot'ko), Naukova Dumka, Kiev (1983).
- ¹⁷J. Friedel, *Dislocations* [Russian transl.], Mir, Moscow (1967).
- ¹⁸S. W. Marx and R. O. Simmons, *J. Chem. Phys.* **81**, 944 (1984).
- ¹⁹*Rare Gas Solids* (ed. by M. L. Klein and J. A. Venables), vol. 1, Acad. Press, London (1976).
- ²⁰D. N. Bol'shutkin and A. I. Prokhvatilov, *Fiz. Tverd. Tela (Leningrad)* **8**, 248 (1966) [*Sov. Phys. Solid State* **8**, 198 (1966)].
- ²¹I. N. Frantsevich, F. F. Voronov, and S. A. Bakuta, *Elastic Constants for Metals and Nonmetals* (A Handbook) [in Russian], Naukova Dumka, Kiev (1982).
- ²²S. Hoen, N. G. Chopra, X.-D. Xiang *et al.*, *Phys. Rev.* **B46**, 12737 (1992).
- ²³D. N. Bol'shutkin, A. V. Leont'eva, V. G. Snigerev, and V. I. Startsev, *Fiz. Tverd. Tela (Leningrad)* **7**, 2607 (1965) [*Sov. Phys. Solid State* **7**, 2110 (1967)].
- ²⁴C. Trepp, *Schweizer Archiv* **24**, 230 (1958).
- ²⁵F. P. Bouden and G. W. Rove, *Proc. Roy. Soc.* **A228**, 1 (1955).
- ²⁶A. I. Prokhvatilov, V. V. Pustovalov, T. V. Sil'vestrova, and V. I. Startsev, *Ukr. Fiz. Zh.* **10**, 1127 (1965).
- ²⁷G. P. Upit and S. A. Varchenya, in: *The Science of Hardness Testing and Its Research Applications* (ed. by J. H. Westbrook and H. Konrad), USA (1971).
- ²⁸M. Haluska, M. Zehetbauer, H. Kuzmany *et al.*, *Mol. Matter* **4**, 73 (1994).
- ²⁹J. Li, T. Mitsuki, M. Ozawa *et al.*, *J. Crystal Growth* **143**, 58 (1994).
- ³⁰N. A. Aksanova, A. P. Isakina, A. I. Prokhvatilov *et al.*, in *Fullerenes. Proc. Symp. on Recent Advances in the Chemistry and Physics of Fullerenes and Related Materials* (ed. by K. M. Kadish and R. S. Ruoff), The Electrochemical Society Inc., Pennington (1994), vol. 94–24.
- ³¹X. D. Shi, A. R. Kortan, J. M. Williams *et al.*, *Phys. Rev. Lett.* **68**, 827 (1992).
- ³²V. S. Bobrov, R. A. Dilanyan, L. S. Fomenko *et al.*, *J. Supercond.* **8**, 1 (1995).
- ³³M. Haluska, M. Zehetbauer, M. Hulman, and H. Kuzmany, in *Materials Science Forum*, vols. 210–213, Part. 1 *Nondestructive Characterization of Materials II* (ed. by A. L. Bartos, R. E. Green, Jr., and C. O. Ruud), Transtec Publ., Switzerland (1966).
- ³⁴G. C. Kuczinski and R. F. Hochman, *Phys. Rev.* **108**, 946 (1957); *Phys. Rev.* **30**, 669 (1959).
- ³⁵Yu. A. Osip'yan, V. F. Petrenko, A. V. Zaretskii, and R. W. Withwort, *Adv. Phys.* **35**, 115 (1986).
- ³⁶J. S. Nadeau, *J. Appl. Phys.* **35**, 669 (1964).
- ³⁷V. I. Orlov, V. I. Nikitenko, R. K. Nikolaev *et al.*, *Pis'ma Zh. Éksp. Teor. Fiz.* **59**, 667 (1994) [*JETP Lett.* **59**, 704 (1994)].
- ³⁸M. Tachibana, H. Sakuma, M. Michiyama, and K. Kojima, *Appl. Phys. Lett.* **67**, 2618 (1995).
- ³⁹B. Ya. Farber, N. S. Sidorov, V. I. Kulakov *et al.*, *Sverkhprovodimost': Fiz., Khim., Tekh.* **4**, 2393 (1991).
- ⁴⁰A. I. Prokhvatilov, I. N. Krupskii, L. D. Yantsevich, and A. S. Baryl'nik, *Pribyora Tekh. Eksper.* No. 3, 261 (1981).
- ⁴¹R. Moret, P. A. Albouy, V. Agafonov *et al.*, *J. Phys. (Paris)* **2**, 511 (1992).
- ⁴²H. Kasatani, H. Terauchi, Y. Hamanaka, and S. Nakashima, *Phys. Rev.* **B47**, 4022 (1993).
- ⁴³G. B. M. Vaughan, Y. Chambre, and D. Dubois, *Europhys. Lett.* **31**, 525 (1995).
- ⁴⁴L. Pintschovius, S. L. Chaplot, G. Roth, and G. Heger, *Phys. Rev. Lett.* **75**, 2843 (1995).
- ⁴⁵H. Klee, H. O. Carmesin, and K. Knorr, *Phys. Rev. Lett.* **61**, 1855 (1988).
- ⁴⁶A. S. Baryl'nik and A. I. Prokhvatilov, *Fiz. Nizk. Temp.* **15**, 971 (1989) [*Sov. J. Low Temp. Phys.* **15**, 536 (1989)].
- ⁴⁷R. Moret, *Phys. Rev.* **B48**, 17619 (1993).
- ⁴⁸K. Sakaue, N. Toyoda, H. Kasatani *et al.*, *J. Phys. Soc. Jpn.* **63**, 1237 (1994).
- ⁴⁹N. Toyoda, K. Sakaue, H. Terauchi *et al.*, *J. Phys. Soc. Jpn.* **63**, 2025 (1994).
- ⁵⁰J. Hirt and I. Lote, *Theory of Dislocations* [Russian transl.], Atomizdat, Moscow (1972).
- ⁵¹Yu. S. Boyarskaya, D. Z. Grabko, and M. S. Kats, *Physics of Microindentation* [in Russian], Shtiintsa, Kishenev (1986).
- ⁵²J. Q. Li, Z. X. Zhao, Y. L. Li *et al.*, *Physica* **C196**, 135 (1992).
- ⁵³H. Werner, M. Wohlers, D. Herein *et al.*, in *Fullerenes and Atomic Clusters, Proc. Intern. Workshop*, St. Petersburg, Russia (1995).
- ⁵⁴W. Schranz, A. Fnith, P. Dolinar *et al.*, *Phys. Rev. Lett.* **71**, 1561 (1993).
- ⁵⁵I. O. Bashkin, N. P. Kobelev, A. P. Moravskii *et al.*, in *Fullerenes and Atomic Clusters, Proc. Intern. Workshop*, St. Petersburg, Russia (1993).
- ⁵⁶P. Bernier, I. Luk'yanchuk, A. Belahmer *et al.*, in *Mat. Res. Soc. Symp. Proc.*, vol. 359 (1995).
- ⁵⁷S. A. Myers, R. A. Assink, J. E. Schirber, and D. A. Loy in *Mat. Res. Soc. Symp. Proc.*, vol. 359 (1995).
- ⁵⁸T. Atake, T. Tanaka, and H. Kawaji, *Chem. Phys. Lett.* **196**, 321 (1992).
- ⁵⁹E. Grivei, M. Cassart, J.-P. Issi *et al.*, *Phys. Rev.* **B48**, 8514 (1993).
- ⁶⁰J. E. Schirber, R. A. Assink, G. A. Samara *et al.*, *Phys. Rev.* **B51**, 15552 (1995).
- ⁶¹H. Warener, D. Bublak, U. Gobel *et al.*, *Angew. Chemie* **31**, 868 (1992).
- ⁶²K. Matsuishi, K. Tada, S. Onari *et al.*, *Phil. Mag.* **B70**, 795 (1994).

Translated by R. S. Wadhwa